

Photonic structures and electromagnetic metamaterials

Petr Kužel (2008–2018)

(Studijní text k přednášce Fotonické struktury a elektromagnetické metamateriály, MFF UK)

Contents

	Page
1 Introduction	1
A Length scales: averaging of electric and magnetic quantities	1
A.1 <i>Atomic scale</i>	1
A.2 <i>Wave equation, plane harmonic waves</i>	2
A.3 <i>Classification of photonic structures</i>	4
B Dispersion curves	8
B.1 <i>Reciprocal space: 1D case</i>	8
B.2 <i>Density of states</i>	11
B.3 <i>Reciprocal space: 2D case</i>	12
2 Propagation in magnetic stratified media	15
A Single interface between homogeneous media	15
A.1 <i>Reflection and refraction at the interface; Snell's law</i>	15
A.2 <i>Fresnel equations</i>	21
A.3 <i>Surface mode</i>	25
B Transfer matrix formalism in magnetic media	29
B.1 <i>Propagation through layered structures</i>	29
B.2 <i>Reflection and transmission coefficients</i>	32
B.3 <i>Fields inside a layered structure</i>	36
B.4 <i>Applications</i>	37
B.5 <i>Guided modes in a layered structure</i>	40
B.6 <i>Transfer matrix of an inhomogeneous slab</i>	42
3 Negative refractive index materials	45
A Historical overview	45
B Negative refraction	46
C Concept of subwavelength focusing	48
C.1 <i>Perfect lens</i>	48
C.2 <i>Silver lens</i>	53
C.3 <i>Near field plates</i>	53
C.4 <i>Epsilon-near-zero media</i>	55
4 Effective properties of composites	57
A General considerations	57
B Maxwell-Garnett model	59
C Bruggeman model	60
D Parallel and serial capacitors	61
E Bergman formulation of effective medium theory	63

5	Effective properties of metamaterials	67
A	Dielectric metamaterials	67
A.1	<i>High-permittivity spheres</i>	67
A.2	<i>High-permittivity rods</i>	75
B	Metallic metamaterials	83
B.1	<i>Array of thin wires</i>	83
B.2	<i>Split-ring resonators</i>	86
B.3	<i>Other designs</i>	87
B.4	<i>Metamaterials: from microwaves to the optical range</i>	91
6	One-dimensional photonic crystals	93
A	Properties of transfer matrices	93
B	Band structure	95
C	Defects and defect modes	101
D	Distribution of the field near the defect	104
E	Manipulation of defect modes	105
E.1	<i>Tuning of defect modes</i>	105
E.2	<i>Amplitude modulation of defect modes</i>	107
7	Numerical methods	115
A	Plane wave expansion	115
B	Transverse matrix method	121
C	Finite-difference time-domain method	123
8	Symmetry of photonic crystals	127
A	Introduction to the group theory	127
B	Application to a 2D photonic crystal with symmetry C_{4v}	131
C	Application to a 3D photonic crystal with simple cubic lattice and symmetry O_h	137
D	Comparison of the photonic crystal and metamaterial approach	140
9	Formal theory of photonic crystals	145
A	Decomposition into the basis of eigen-functions	145
B	Green's function	147
C	Solution of the wave equation with the right-hand-side	148
D	Spontaneous emission	149
E	Defect modes	151
F	Stimulated emission	153
G	Nonlinear phenomena: sum frequency generation	155

1. Introduction

A. Length scales: averaging of electric and magnetic quantities

A.1. Atomic scale

The classical electromagnetic theory describes the electromagnetic field and its interaction with the matter which consists, on an atomic scale, of an ensemble of charged particles. The field which enters into play is local and it may vary by many orders of magnitude on an inter- and intra-atomic scale (namely in the vicinity of charges). The coupling between charges and the field is described by Maxwell-Lorentz equations for the local electric field \mathbf{e} and magnetic induction \mathbf{b} :

$$\nabla \cdot \mathbf{e} = \frac{\rho}{\varepsilon_0} \tag{1.1a}$$

$$\nabla \cdot \mathbf{b} = 0 \tag{1.1b}$$

$$\nabla \times \mathbf{e} + \frac{\partial \mathbf{b}}{\partial t} = 0 \tag{1.1c}$$

$$\frac{1}{\mu_0} \nabla \times \mathbf{b} - \varepsilon_0 \frac{\partial \mathbf{e}}{\partial t} = \mathbf{j}, \tag{1.1d}$$

where \mathbf{j} and ρ denote the local current and density of charge, respectively. Employing the classical mechanics view of point charges, these quantities have a discrete nature expressed by Dirac δ -functions:

$$\rho(\mathbf{r}, t) = \sum_{\alpha} q_{\alpha} \delta(\mathbf{r} - \mathbf{r}_{\alpha}(t)), \tag{1.2a}$$

$$\mathbf{j}(\mathbf{r}, t) = \sum_{\alpha} q_{\alpha} \delta(\mathbf{r} - \mathbf{r}_{\alpha}(t)) \mathbf{v}_{\alpha}(t). \tag{1.2b}$$

The solution of the electromagnetic problem, *i.e.*, of equations (1.1) and (1.2) supplemented by the Lorentz force $\mathbf{f} = \rho \mathbf{e} + \mathbf{j} \times \mathbf{b}$ on a macroscopic scale, would imply finding the positions (and their time evolution) of a huge number of charges. This is not feasible and also such detailed information is not needed for practical applications. It is then convenient to proceed to a space averaging of the local quantities on the atomic scale. The appropriate scale for this averaging is ~ 10 nm, which means that this concept is valid up to the frequencies of radiation in the vacuum UV spectral range ($\lambda \gg 10$ nm). The local response of charges (the current of free charges and the dipolar polarization of the bound charges) then can be taken into account by complex and frequency-dependent material parameters ε (dielectric permittivity) and μ (magnetic permeability) which describe the macroscopic polarization \mathbf{P} and magnetization \mathbf{M}

of the medium and connect the spatially averaged vector fields $\mathbf{E} = \langle \mathbf{e} \rangle$ and $\mathbf{B} = \langle \mathbf{b} \rangle$ to newly introduced vectors \mathbf{D} and \mathbf{H} through the so called constitutive relations:

$$\mathbf{D}(\omega) = \varepsilon(\omega)\varepsilon_0\mathbf{E}(\omega) = \varepsilon_0\mathbf{E} + \mathbf{P} \quad (1.3a)$$

$$\mathbf{B}(\omega) = \mu(\omega)\mu_0\mathbf{H}(\omega) = \mu_0(\mathbf{H} + \mathbf{M}), \quad (1.3b)$$

which should satisfy the Maxwell equations for macroscopic fields¹:

$$\nabla \cdot \mathbf{D} = 0 \quad (1.4a)$$

$$\nabla \cdot \mathbf{B} = 0 \quad (1.4b)$$

$$\nabla \times \mathbf{E} + \frac{\partial \mathbf{B}}{\partial t} = 0 \quad (1.4c)$$

$$\nabla \times \mathbf{H} - \frac{\partial \mathbf{D}}{\partial t} = 0. \quad (1.4d)$$

The quantities \mathbf{e} and \mathbf{b} contain the near-field information, i.e., the variation of local fields on the atomic scale, while the vectors \mathbf{E} , \mathbf{D} , \mathbf{H} , \mathbf{B} describe correctly the far field but we cannot use them to retrieve the near field.

Note that in this textbook we use the convention where the harmonic wave in the complex notation is described by the phase factor $e^{+i\omega t}$ and the complex material response is then given by $\varepsilon = \varepsilon' - i\varepsilon''$, $\mu = \mu' - i\mu''$.

A.2. Wave equation, plane harmonic waves

The Maxwell equations along with the constitutive relations represent a set of coupled differential equations for four field vectors. It would be then convenient to derive equations which determine each of the field vectors separately. We consider an angular frequency component ω , we apply the *curl* operator ($\nabla \times$) to (1.4c) and the operator $\partial/\partial t$ to (1.4d); comparing the two resulting relations we obtain:

$$\nabla \times \frac{1}{\mu}(\nabla \times \mathbf{E}) - \frac{\omega^2}{c^2}\varepsilon\mathbf{E} = 0. \quad (1.5)$$

Similarly, one may find for the magnetic field:

$$\nabla \times \frac{1}{\varepsilon}(\nabla \times \mathbf{H}) - \frac{\omega^2}{c^2}\mu\mathbf{H} = 0. \quad (1.6)$$

In the general case we cannot simplify these equations further because we wish to study inhomogeneous media (i.e., both μ and ε can depend on \mathbf{r}).

Homogeneous case In the homogeneous case the solutions of wave equations are the plane monochromatic waves:

$$\mathbf{E} = \mathbf{E}_0 e^{i(\omega t - \mathbf{k} \cdot \mathbf{r})}, \quad \mathbf{H} = \mathbf{H}_0 e^{i(\omega t - \mathbf{k} \cdot \mathbf{r})}; \quad (1.7)$$

the angular frequency ω and the wave vector \mathbf{k} being connected by

$$|\mathbf{k}|^2 \equiv k^2 = \varepsilon\mu \frac{\omega^2}{c^2}. \quad (1.8)$$

We can introduce the complex refractive index $N = n - i\kappa$

$$k = \frac{\omega}{c}N. \quad (1.9)$$

¹Note that we can—without losing the general character of the solutions of Maxwell equations—omit the current density in (1.4d) and the density of free charges in (1.4a). We just need to postulate that all the effects related to both bound and free charges are described by a complex dielectric permittivity ε .

Back to the Maxwell equation (1.4c), using plane monochromatic wave solution we obtain

$$i\mathbf{k} \times \mathbf{E}_0 = i\omega\mu\mu_0\mathbf{H}_0, \quad (1.10)$$

or, by substituting the unit vector in the propagation direction $\mathbf{s} = \mathbf{k}/k$:

$$\mathbf{H}_0 = \sqrt{\frac{\varepsilon_0}{\mu_0}} \sqrt{\frac{\varepsilon}{\mu}} (\mathbf{s} \times \mathbf{E}_0). \quad (1.11)$$

The vectors \mathbf{k} , \mathbf{E} , and \mathbf{H} form a right-handed basis and it follows that \mathbf{H}_0 (and \mathbf{B}_0) are unambiguously determined by \mathbf{k} and \mathbf{E}_0 . We define the vacuum wave impedance η_0 and the relative wave impedance Z :

$$\eta_0 = \sqrt{\frac{\mu_0}{\varepsilon_0}} \approx 377 \Omega, \quad (1.12)$$

$$Z = \sqrt{\frac{\mu}{\varepsilon}} \quad (1.13)$$

we thus obtain the following relations for the field amplitudes:

$$\frac{E_0}{H_0} = \sqrt{\frac{\mu_0}{\varepsilon_0}} \equiv \eta_0, \quad \frac{E_0}{B_0} = \sqrt{\frac{1}{\mu_0\varepsilon_0}} \equiv c. \quad (1.14)$$

The plane harmonic waves form a complete orthogonal basis; consequently, any solution of the wave equation can be expressed as a linear combination of these modes. The time domain shaping of optical pulses can be described by the integral

$$\mathbf{E}(\mathbf{r}, t) = \int \mathbf{E}(\mathbf{r}, \omega) e^{i\omega t} dt \quad (1.15)$$

and the distribution of the field in the space can be defined using integration over the wave vector \mathbf{k} :

$$\mathbf{E}(\mathbf{r}, t) = \iiint \mathbf{E}(\mathbf{k}, \omega) e^{i(\omega t - \mathbf{k} \cdot \mathbf{r})} d\mathbf{k}, \quad (1.16)$$

where we must keep in mind the relation (1.8) between ω and \mathbf{k} .

Inhomogeneous case: Maxwell equations feature the so called scaling property, which means that if an inhomogeneity is scaled in the space the electromagnetic waves behave in exactly the same manner on both scales providing that the wavelength (frequency) is also appropriately scaled. Let us introduce a scaling by a coefficient a :

$$\frac{1}{a}\mathbf{r} = \mathbf{r}'. \quad (1.17)$$

The inhomogeneous properties of the permittivity and permeability are scaled by this factor:

$$\tilde{\varepsilon}(\mathbf{r}') = \varepsilon(\mathbf{r}), \quad \tilde{\mu}(\mathbf{r}') = \mu(\mathbf{r}). \quad (1.18)$$

We introduce a scaled frequency $\omega' = a\omega$ and the nabla operator scales in the following way: $\nabla' = a\nabla$. We formally define the field in the new coordinates: $E'(\mathbf{r}', \omega') = E(\mathbf{r}, \omega)$. The wave equation (1.5)

$$\frac{1}{\varepsilon} \nabla \times \frac{1}{\mu} [\nabla \times \mathbf{E}(\mathbf{r}, \omega)] = \frac{\omega^2}{c^2} \mathbf{E}(\mathbf{r}, \omega) \quad (1.19)$$

will read after the scaling substitution

$$\frac{1}{\tilde{\varepsilon}} \frac{1}{a} \nabla' \times \frac{1}{\tilde{\mu}} \left[\frac{1}{a} \nabla' \times \mathbf{E}'(\mathbf{r}', \omega') \right] = \frac{\omega'^2}{c^2} \mathbf{E}'(\mathbf{r}', \omega'), \quad (1.20)$$

i.e.

$$\frac{1}{\tilde{\varepsilon}} \nabla' \times \frac{1}{\tilde{\mu}} [\nabla' \times \mathbf{E}'(\mathbf{r}', \omega')] = \frac{\omega'^2}{c^2} \mathbf{E}'(\mathbf{r}', \omega'), \quad (1.21)$$

which does not depend on a . We conclude: one obtains the same electromagnetic properties of an inhomogeneous structure in two different spectral regions by an appropriate scaling of its dimensions providing that the values of ε and μ are the same in these frequency regions.

In periodic media the propagation of electromagnetic waves will be described by a wave vector \mathbf{k} . We will introduce the dimensionless quantities $\mathbf{K} = \mathbf{k}a/(2\pi)$ and $\Omega = \omega a/(2\pi c)$; by means of these quantities the electromagnetic properties of any structure can be described in a general manner without introducing any characteristic length scale. All equivalent structures (obtained only by scaling) will have the same properties in an appropriately scaled frequency range.

A.3. Classification of photonic structures

The dielectric polarization of media is connected to a dynamical separation of bound charges which define the electric dipole moments; the magnetic polarization in materials then arises from the orbital currents or from unpaired electron spins. The characteristic distances and sizes of the current loops are then on sub-nm scale which may impose some limits to the strength of the resonant interaction with the field. Namely, the resonant phenomena in magnetic systems tend to occur in the microwave range which results in an absence (or at least weakness) of the natural magnetic material response at THz and higher frequencies.

Patterning the materials brings another length scale into play. The macroscopic fields on the atomic scale may now regain a local character with respect to the length scale of the newly introduced inhomogeneity (artificial structure). We assume this structure periodic; the size of the unit cell is chosen to be substantially smaller than the targeted wavelength and, at the same time, much larger than the interatomic distances. Patterns within the unit cell of such a structure can be considered as artificial "meta-atoms" characterized by electric and magnetic dipole moments. These dipole moments are now defined not only by the materials used but also by the geometry of the artificial structure, i.e., by the extent of the possible charge separation and by the area of the surface delimited by the current loops. On the one hand, at the length scale of the wavelength the meta-atoms constitute elementary electric and magnetic dipole moments which can be macroscopically described by effective permeability and permittivity obtained by an averaging procedure (analogous to that used at the atomic scale); on the other hand, the magnitudes of the dipoles may significantly exceed those observed on the atomic scale and the positions of the resonant frequencies can be tailored by the geometry and the length scale of the structure.

The very important parameters are the dimensions of the unit cell and of the individual meta-atoms (denoted by l and D , respectively, in the schemes in Table 1.1) or, more precisely, their ratios to the wavelength. We may distinguish three different regimes which are described below and summarized in Table 1.1.

Composites By composites we mean here the structures which can be described within a static approximation which involves the standard effective medium theory (column 3 in Table 1.1). For example, if we consider a purely dielectric composite, then the electromagnetic field can be considered as almost homogeneous inside the dielectric inclusions. This is expressed by the conditions for the applicable radiation wavelengths $\lambda \gg \sqrt{\varepsilon_2}l$ and $\lambda \gg \sqrt{\varepsilon_1}D$ in Table 1.1.

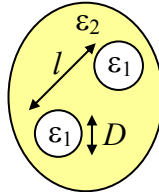
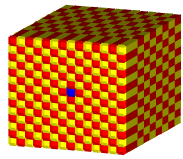
Category	Atomic scale ~ 10 nm	Composites	Metamaterials	Photonic crystals
Scheme				
microscopic description	e, b	Dielectric or metallic inclusions: l, D, ϵ_i (or σ_i)		periodic ϵ
macroscopic description	averaging: E, B, D, H	EMA (Maxwell-Garnett, Bruggeman...)	Extension of EMA (Mie scattering theory) other homogenization procedures	Band structure
validity of macroscopic description	$\lambda \gg 10 \text{ nm}$	$\lambda \gg \sqrt{\epsilon_2} l, \sqrt{\epsilon_2} D$ $\lambda \gg \sqrt{\epsilon_1} D$	$\lambda \gg \sqrt{\epsilon_2} l, \sqrt{\epsilon_2} D$ $\lambda \approx \sqrt{\epsilon_1} D$	$\lambda \approx \sqrt{\epsilon} l$
effective parameters	ϵ, μ	ϵ_{eff} ($\mu_{\text{eff}} = 1$)	$\epsilon_{\text{eff}}, \mu_{\text{eff}}$	—
origin of resonant behaviour	polarization of bound charges orbital currents, spins	Dielectrics: no geometrical resonance Metals: plasmonic resonance	each element is individually resonant no coupling between elements	resonances due to interferences coupling between periodically distributed elements
reciprocal space (reciprocal parameter G)	—	$0 \approx \omega/c \ll G$	below the first bandgap $\omega/c < G$	Band structure with bandgaps spatial dispersion of the photonic crystal

Table 1.1: Inhomogeneities on various length scales compared to the wavelength and their description. (EMA = effective medium approximation)

We do not expect any additional geometry-related resonances in this spectral range and the medium can be described by effective medium approximation (EMA). Within this approximation the effective permittivity of the composite is evaluated in terms of the dielectric functions of the components, of their shape and of their volume fractions. No anomaly of the magnetic permeability is expected here ($\mu_{\text{eff}} \approx 1$) if we deal with intrinsically non-magnetic components. The two most widely used effective medium models are the Maxwell-Garnett model and the Bruggeman model described in Chapter 3 of this textbook.

The effective medium approach can be also used for metal-dielectric composites with very small metallic particles where the conductivity (connected to the imaginary part of the permittivity) of inclusions dominates. The condition $\lambda \gg |\sqrt{\epsilon_1}|D$ in a metal leads then essentially to the requirement that the metallic particle size is much smaller than the electromagnetic skin depth. Then the details of the metal structure are too small to lead to shape-dependent resonances in the targeted spectral range (the condition $\lambda \gg c\sqrt{L_{\text{int}}C_{\text{int}}}$ is satisfied, where L_{int} and C_{int} are internal inductance and capacitance of a meta-atom which are related to its shape and morphology).

The response of sub-wavelength metallic particles is very specific and different from that of dielectric particles. This is related to the fact that the metallic conductivity inherently involves the plasmonic resonance which has a longitudinal character in a homogeneous medium (the frequency of the corresponding transverse resonance of charge carrier motion vanishes due

to the lack of the restoring force). Inhomogeneities introduced in the medium then lead to the occurrence of a restoring force owing to the charge separation. In other words, the sub-wavelength metallic particles exhibit a high dipolar polarizability which depends on their size. The applied optical electric field then can induce charges at their edges which lead to a high effective dipole moment of the particles and a transverse plasmonic resonance may appear in ϵ_{eff} in the target frequency range. The plasmonic resonance is not critically dependent on the shape of meta-atoms and it is essentially due to the nature of metallic conductivity; for this reason it can be described by a standard EMA in analogy with the dielectrics.

Metamaterials In the metamaterials the electromagnetic field is inhomogeneously distributed within the fine details of the unit cell structure. The incident radiation scatters on the pattern and gives rise to the resonances which are closely connected to this inhomogeneous distribution of the local field. In principle, each scattering element is individually resonant and no interaction (interference) between the neighboring unit cells needs to be considered in order to obtain the effective resonant behavior (in practice, weak coupling between neighboring elements always exists). Strictly speaking, as the interaction between the meta-atoms is negligible, their periodic distribution is not required and a structure with some degree of randomization of the position of meta-atoms should exhibit a very similar response to an exactly periodic structure. However, in this textbook we will most often assume that the metamaterial pattern is periodic; this assumption is compatible with many technological processes (lithographic deposition, etching etc.) which usually provide periodic structures and it also allows us to benefit of the notion of the unit cell and of the related description in the reciprocal space.

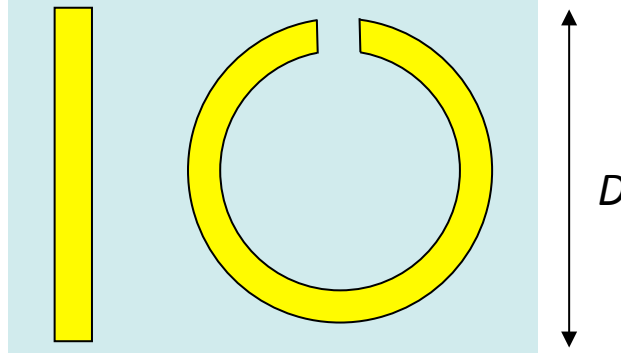


Figure 1.1: Example of meta-atoms—building blocks of a metamaterial; $D \ll \lambda$. Such patterns introduce new electric and magnetic dipoles on the wavelength scale.

We deal with dielectric or metallic inclusions (scatterers) forming a motive of the structure characterized by a high permittivity or conductivity, *i.e.*, $|\epsilon_1| \gg |\epsilon_2|$. The size of the individual scatterers is much smaller than the wavelength of the probing radiation in vacuum (or in the surrounding medium 2). This enables a procedure of homogenization of ϵ and μ in the sample, *i.e.*, attribution of effective permeability and permittivity to the metamaterial. These effective parameters must then be able to describe the electromagnetic properties of the metamaterial from the macroscopic point of view (transmission and reflection of the radiation).

The spatial distribution of the near field can be used, as originally proposed by Pendry, for evaluation of the effective properties of the medium. The tensors of effective permittivity and permeability of the metamaterial are defined as the ratios of suitably averaged electric and

magnetic displacements and fields:

$$\varepsilon_{ij,\text{eff}} = \frac{\langle D_i \rangle}{\langle E_j \rangle}, \quad (1.22a)$$

$$\mu_{ij,\text{eff}} = \frac{\langle B_i \rangle}{\langle H_j \rangle}, \quad (1.22b)$$

where the averaging procedures were inspired by the integral form of the Maxwell equations:

$$\oint_c \mathbf{E} \cdot d\mathbf{l} = -\frac{\partial}{\partial t} \int_S \mathbf{B} \cdot d\mathbf{S}, \quad (1.23a)$$

$$\oint_c \mathbf{H} \cdot d\mathbf{l} = \frac{\partial}{\partial t} \int_S \mathbf{D} \cdot d\mathbf{S}. \quad (1.23b)$$

Here the fields are integrated over closed loops while the displacements are integrated over surfaces delimited by these contours. Thus the macroscopic electric and magnetic fields $\langle \mathbf{E} \rangle$ and $\langle \mathbf{H} \rangle$ need to be calculated as average values along a curve. Pendry et al. [J. B. Pendry et al., IEEE Trans. Microw. Theory Tech. 47, 2075 (1999)] have proposed to average local field values along Cartesian axes of the unit cell with dimensions $a \times b \times c$ (which is chosen such that the contour does not intersect the enclosed metamaterial pattern), *e.g.*,

$$\langle H \rangle_x = \frac{1}{a} \int_{(0,0,0)}^{(a,0,0)} \mathbf{H} \cdot d\mathbf{r}. \quad (1.24)$$

In contrast, the components of the electric and magnetic displacements \mathbf{D} and \mathbf{B} are averaged over the faces of the unit cell:

$$\langle B \rangle_x = \frac{1}{b \times c} \int_{S_{yz}} \mathbf{B} \cdot d\mathbf{S}. \quad (1.25)$$

The inhomogenous distribution of the electromagnetic field inside the unit cell practically does not influence the average value of the fields while it strongly affects the average value of the displacement vectors. In this sense, highly inhomogeneous distribution of the near-field, reflecting a strong interaction of the radiation with the metamaterial pattern (a weak interaction would not significantly change a quasi-homogeneous character of the incident plane wave within the unit cell) may lead to high values of ε_{eff} and/or μ_{eff} which, in turn, describe the resonant electromagnetic behavior of the structure. This rather heuristic averaging procedure has been originally developed for metallic scatterers but it has been successfully used also in the case of dielectric resonators. With metals it is possible to deposit planar (or even layered) structures on a substrate such that their geometrical shape maximizes the electric and/or magnetic response, *i.e.*, the charge separation (electric dipole) and the current loop (magnetic dipole). The details of the shape of such metallic inclusions then define the resonance frequency and the resonant strength. The magnetic dipole moment is related to the currents flowing along metallic rings and it can be induced if the magnetic field of the incident radiation points through the ring.

Photonic crystals As already pointed out, in the case of metamaterials the periodicity of the structural pattern is not a requirement; each scattering element is individually resonant and the interaction between the neighboring unit cells is weak. On the other hand, if the radiation wavelength becomes comparable to (or even smaller than) the characteristic distances in the structure, interferences between scattered (partially reflected and diffracted) waves become an important issue: the category of photonic crystals shown in the last column of Table 1.1 has only sense if we consider periodic structures. The condition $\lambda \approx \sqrt{\varepsilon}l$ then ensures

that constructive and destructive interference phenomena may occur in the relevant frequency range for some propagation and scattering directions. This leads to the formation of a photonic band structure.

Let us define the periodicity of the dielectric or magnetic properties by the vector $\mathbf{R} = m\mathbf{a} + n\mathbf{b} + l\mathbf{c}$, where \mathbf{a} , \mathbf{b} , and \mathbf{c} are the vectors of the unit cell and m , n , and l are integers. It means that $\varepsilon(\mathbf{r} + \mathbf{R}) = \varepsilon(\mathbf{r})$, $\mu(\mathbf{R} + \mathbf{r}) = \mu(\mathbf{r})$. In a periodic medium the field distribution can be described by the Bloch theorem: the mode with the wave vector \mathbf{k} is given by the product of a plane wave and of a periodic function (with the same periodicity \mathbf{R} as the permittivity and/or permeability of the photonic structure); e.g., we can write for the electric field oscillating at frequency ω :

$$\mathbf{E}_{\mathbf{k}}(\mathbf{r}, t) = \exp(i\omega t) \exp(-i\mathbf{k} \cdot \mathbf{r}) \sum_{\mathbf{G}} \mathbf{e}_{\mathbf{k}, \mathbf{G}} \exp(-i\mathbf{G} \cdot \mathbf{r}), \quad (1.26)$$

where \mathbf{G} are vectors of the reciprocal lattice whose definition is: $\mathbf{G} \cdot \mathbf{R} = 2\pi p$ (p is an integer). This condition ensures that the function defined by the sum is periodic as required and its shape is defined by the coefficients $\mathbf{e}_{\mathbf{k}, \mathbf{G}}$ of the Fourier series. The above equation means that the Bloch wave is a linear combination of plane waves with wave vector \mathbf{k} , $\mathbf{k} + \mathbf{G}$, $\mathbf{k} - \mathbf{G}$, \dots :

$$\mathbf{E}_{\mathbf{k}}(\mathbf{r}, t) = \exp(i\omega t) \sum_{\mathbf{G}} \mathbf{e}_{\mathbf{k}, \mathbf{G}} \exp[-i(\mathbf{k} + \mathbf{G}) \cdot \mathbf{r}], \quad (1.27)$$

The sum runs over all reciprocal lattice vectors \mathbf{G} and we now understand that we cannot distinguish between modes with the wave vectors \mathbf{k} and $\mathbf{k} + \mathbf{G}$, *etc.* and new eigenmodes are defined by their particular linear combinations given by (1.27). These linear combinations will form bands of the photonic crystal.

B. Dispersion curves

B.1. Reciprocal space: 1D case

These considerations lead us to the notion of the reciprocal space (space of wave vectors \mathbf{k}) and to the dispersion curves: $\omega(\mathbf{k})$ dependences. Let us first consider waves in a homogeneous space. The dispersion curve is given by (1.9):

$$\mathbf{K} = n\Omega, \quad (1.28)$$

i.e., it is a straight line as shown in Fig. 1.2(a). Now let us introduce an infinitesimal spatial periodic perturbation of the permittivity in one dimension: $\varepsilon(x + mX) = \varepsilon(x)$. The periodic character of the perturbation leads us to the Bloch wave solution (1.27); it means that the modes separated by the reciprocal lattice parameter $G = 2\pi/X$ become coupled. These coupled modes related to one specific value of the wave vector \mathbf{k} are shown by full circles in Fig. 1.2. Their coupling makes an equivalence between all the wave vectors which are separated by the reciprocal lattice vectors. It is then possible to reduce the reciprocal space into a single Brillouin zone by folding the dispersion curves as in Fig. 1.2(b): all the coupled modes then possess the same wave vector \mathbf{k} .

We then increase the magnitude of the perturbation. This starts to renormalize the eigenfrequencies of the coupled modes and lifts the mode degeneracy at the Brillouin zone boundary, see Fig. 1.3. In this way the photonic bands are formed and the forbidden bands (band gaps) appear in between. As an example, we show in Fig. 1.4 the distribution of the electric field in a one-dimensional photonic structure at the Brillouin zone boundary corresponding to Fig. 1.3(a) and (b). In both cases the degeneracy is lifted at the 1 BZ boundary. The low-frequency branch of the dispersion curve is called the “dielectric” branch because the electric field is concentrated

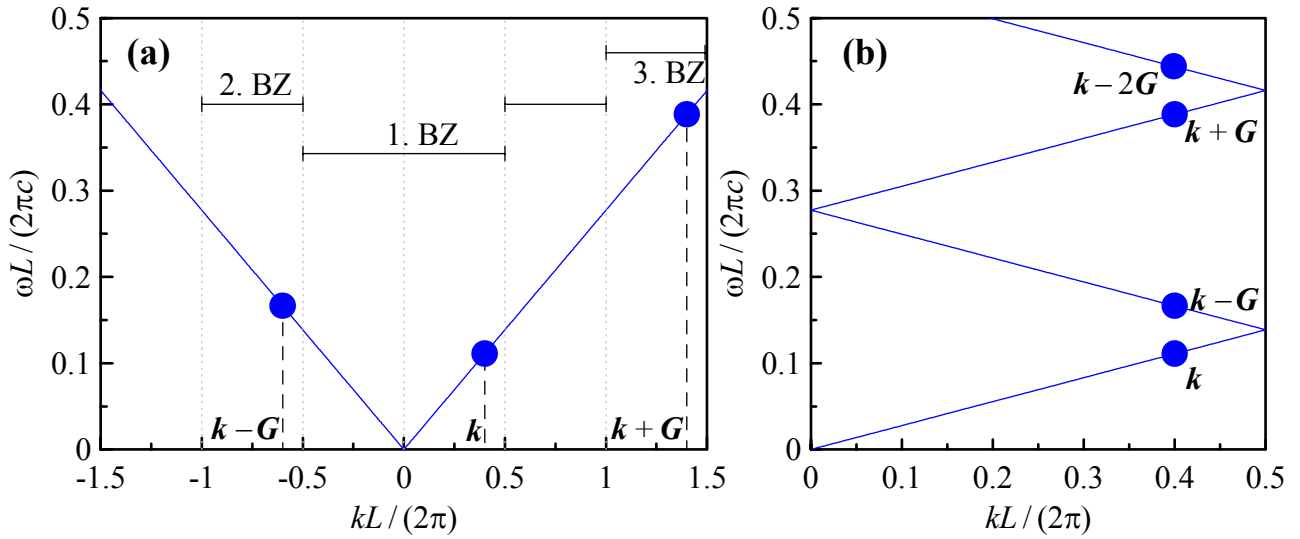


Figure 1.2: (a) Dispersion of electromagnetic waves in the free space (with $\varepsilon = 13$, $\mu = 1$). The modes marked by symbols couple together when an infinitesimal periodic perturbation of the permittivity (with a period L) is switched on. (b) Dispersion curves folded into the first Brillouin zone (1. BZ). In this representation the coupled modes possess the same wave vector \mathbf{k} .

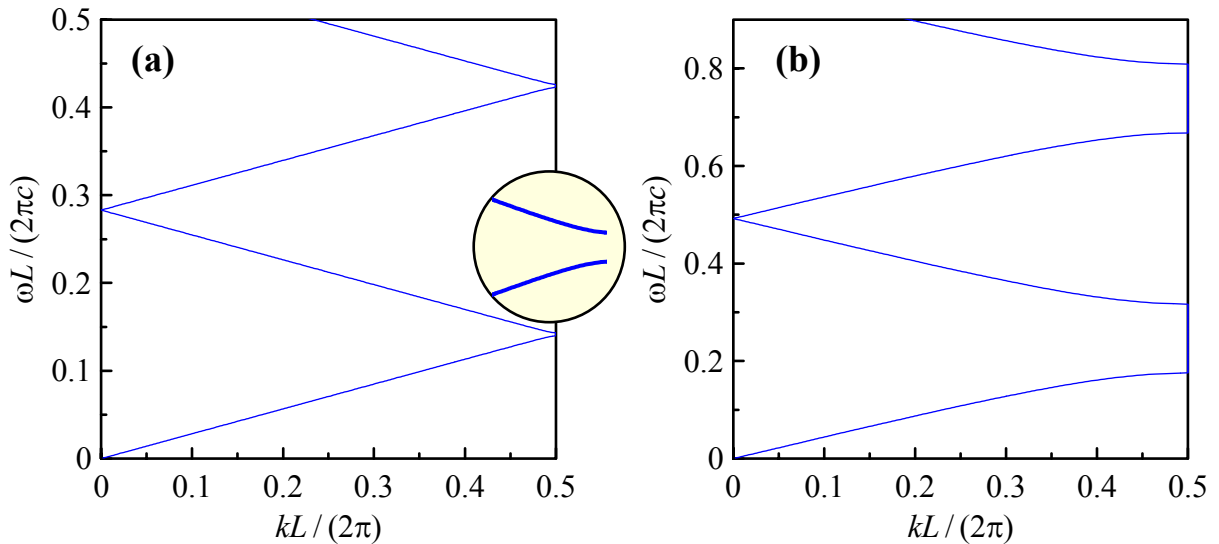


Figure 1.3: (a) Dispersion of a one-dimensional photonic crystals consisting of a periodically repeated bilayer AB with $\varepsilon_A = 13$, $\varepsilon_B = 12$ and period L . A band gap (frequency band with no photonic states) opens at the Brillouin zone boundary $K \equiv kL/(2\pi) = 0.5$. (b) Dispersion of a similar photonic crystal with $\varepsilon_A = 13$, $\varepsilon_B = 2$: a higher contrast of dielectric properties leads to the widening of the band gap.

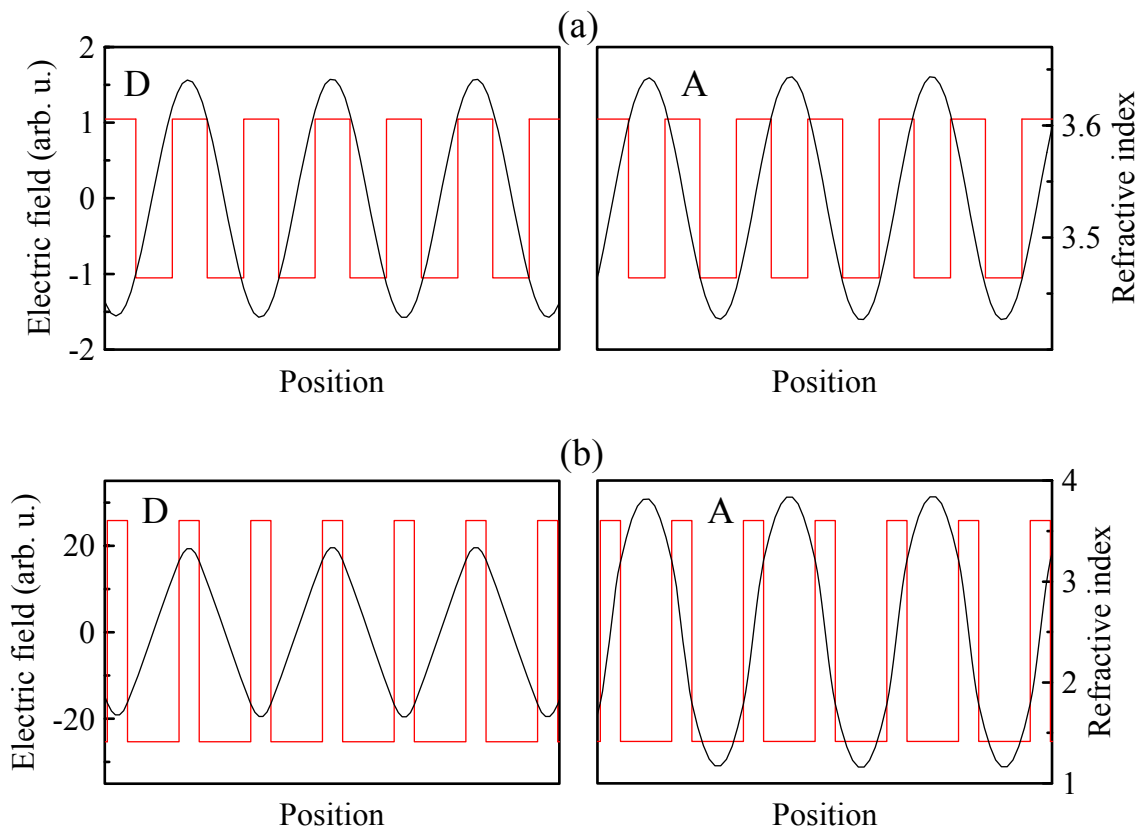


Figure 1.4: Field distribution in a one-dimensional photonic crystal at the Brillouin zone boundary for the low-frequency “dielectric” branch (D) and high-frequency “air” branch (A). These modes correspond to the dispersion curves shown in Fig. 1.3. Red lines show the spatial variation of the refractive index. (a) $\varepsilon_A = 13$, $\varepsilon_B = 12$. (b) $\varepsilon_A = 13$, $\varepsilon_B = 2$. For a small contrast between the permittivities (a) the field distribution is close to a sinusoidal wave; for a high contrast between the permittivities (b) the modes in the Bloch sum (1.26) are more strongly coupled which has as consequence a wider forbidden band and a significantly distorted field distribution.

mainly in the high-permittivity parts of the photonic crystal (curves denoted as D in Fig. 1.4). The field has nodes in the low-permittivity part of the photonic crystal.

In fact, in analogy with the quantum mechanics, the function $1/\varepsilon(\mathbf{r})$ can be considered as a potential and the frequency ω represents the energy. If the field is concentrated namely in the regions with a low potential (high permittivity values), we obtain a lower energy of the system (lower frequency) and vice versa. The upper dispersion branches are called “air” branches and the field here concentrates in the low-permittivity part of the photonic structure (which is most frequently air in real photonic crystals).

This is quite a general property of photonic crystals; it can be also compared to a basic finding of the eikonal theory of the geometrical optics: the beam always bends towards the high-permittivity part of the space, *i.e.*, a high-permittivity region constitutes an “attractive potential” for the field.

From the point of view of the dispersion curves in the reciprocal space, the spectral domain where the periodic photonic structure can be described as a metamaterial remains on the lowest dispersion branch below the first band gap; the condition $\lambda \gg \sqrt{\varepsilon_2}l$ is equivalent to $\omega/c \ll G$ (where G is the reciprocal lattice parameter of the periodic photonic structure), *i.e.*, we deal with the wave vectors well below the Brillouin zone boundary. As the characteristic dimensions

of the structure increase above the value of $\lambda/10$ (we get closer to the Brillouin zone boundary), the homogenization of the medium may progressively become possible only if we admit the spatial dispersion (*i.e.*, a dependence of ε_{eff} and μ_{eff} on the wave vector), which is a consequence of the non-local character of the response of the structure and which is in agreement with the existence of a band structure (the propagation of light cannot be simply described by a refractive index value but a complex band structure of the photonic crystal must be considered). In the metamaterial regime the lowest dispersion branch (*i.e.* the only one which fulfills the condition $\omega/c \ll G$) is quite weakly coupled to the other branches via the Bloch sum since it is well separated from the other branches in the frequency space. The metamaterial resonance then cannot be related to collective phenomena (interferences within the photonic structure) but arises due to the resonant behavior of the metamaterial motive (each metamaterial element is individually resonant).

B.2. Density of states

The photonic crystals offer a possibility to design and modify the density of states $\varrho(\omega)$ of the radiation. For example, the forbidden bands do not exhibit any propagative photonic state, while some photonic bands can feature an enhanced density of states. The radiation properties of molecules and atoms then strongly depend on the density of states of the surrounding photonic structure since it influences both the spontaneous and stimulated emission. Consider an atom embedded in a photonic crystal with a radiation frequency falling into the band gap; its spontaneous emission is then inhibited (or at least strongly suppressed), due to the photonic properties of the environment.

To calculate the number of states within some volume in the \mathbf{k} space we need to discretize the values of the wave vector. This is usually done by imposing periodic boundary conditions; *e.g.* in 1D:

$$E_k(x + L) = \exp(-ikL)E_k(x) = E_k(x), \quad (1.29)$$

where $L = mX$, m being an arbitrarily chosen large integer. The first equality in (1.29) just expresses the Bloch theorem and the second equality provides a discretization of k :

$$k = \frac{2\pi p}{L}. \quad (1.30)$$

where p is another integer. The range in the k -space occupied by a single value of the discretized wave vector is then $2\pi/L$. Similarly, in the 3D case, the volume occupied by a single discrete k -value is $(2\pi)^3/V$, where $V = L_1L_2L_3$ is a (large) volume where the periodic boundary conditions have been imposed.

The density of states $\varrho(\omega)$ is defined as the number of states at frequency ω per unit frequency. It means that the number of states in a small spectral range $\Delta\omega$ is equal to $\varrho(\omega)\Delta\omega$. The states in the \mathbf{k} -space form a mesh with equidistant spaces, as pointed out above; in the frequency domain the states are not equidistant in general and their distribution (density) depends on the dispersion $\omega(\mathbf{k})$. For an example in the free space (with the dispersion $\omega = c|\mathbf{k}| \equiv ck$) the states in the range $(\omega, \omega + \Delta\omega)$ lie within a spherical shell with the \mathbf{k} -space volume

$$\Delta K = 4\pi k^2 \frac{dk}{d\omega} \Delta\omega = 4\pi \frac{\omega^2}{c^3} \Delta\omega. \quad (1.31)$$

The number of states within this shell is $2\Delta K \times V/(2\pi)^3$, where the factor 2 takes into account the double degeneracy of the dispersion curve (two orthogonal polarization states). We find that the density of states per unit volume V is equal to

$$\varrho(\omega) = \frac{\omega^2}{\pi^2 c^3}. \quad (1.32)$$

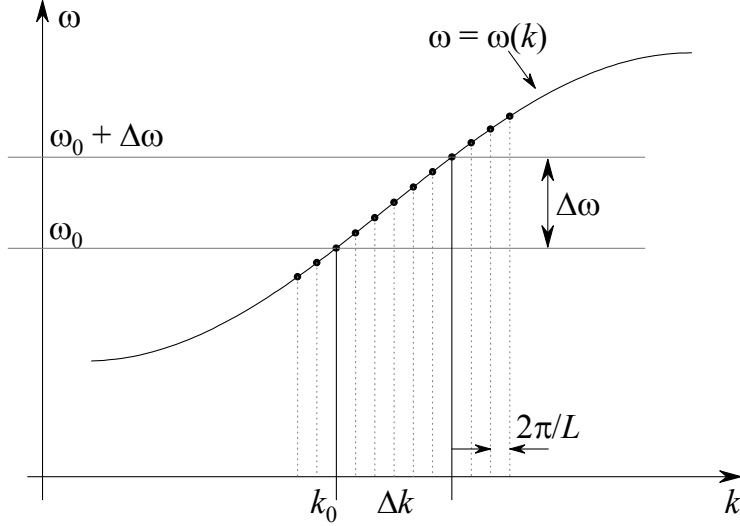


Figure 1.5: Illustration of the density of states for the dispersion $\omega(k)$ in a 1D system. The spacing between the neighboring k -values is equidistant, while that of ω -values is not. The mapping of Δk onto $\Delta\omega$ provides the density of states.

In the case of the photonic crystal we usually need to evaluate the density of states belonging to some particular band $\omega_n(\mathbf{k})$. 1D case is schematically shown in Fig. 1.5. The number of states within the range Δk is $\Delta k \times L/(2\pi) = \varrho(\omega)\Delta\omega$. From that we easily find that the density of states per unit length L depends on the group velocity of light on this branch:

$$\varrho(\omega) = \frac{1}{2\pi} \frac{1}{d\omega(k)/dk}; \quad (1.33)$$

in particular, a “slow light” with very flat dispersion curve exhibits a high density of states.

The situation is quite analogous in the 3D case; however, the complicated topology of the problem usually requires a numerical calculation of the density of states (using calculations based *e.g.* on Monte-Carlo algorithms). It is necessary to evaluate the volume in the \mathbf{k} -space delimited by frequencies ω and $\omega + \Delta\omega$ on the dispersion curve. We can state in general that flat bands (and namely those close to the 1 BZ boundary) will be associated with a large volume in the k -space and, consequently, with a large density of states.

B.3. Reciprocal space: 2D case

We consider here an array of cylindrical dielectric rods forming a 2D photonic structure with a square unit cell and a lattice parameter a as depicted in Fig. 1.6(a). In the reciprocal space we obtain also a square lattice with the reciprocal lattice vectors $\mathbf{G}_1 = (2\pi/a, 0)$ and $\mathbf{G}_2 = (0, 2\pi/a)$. In Fig. 1.6(a) we see some specific points in the reciprocal space: $\Gamma = (0, 0)$, $X = (\pi/a, 0)$, $M = (\pi/a, \pi/a)$. The lines $\Delta = (k_x, 0)$ and $\Sigma = (k_x, k_x)$ make connections between them. The points M and X lie at the first Brillouin zone boundary [dotted line in Fig. 1.6(a)].

The dispersion curve in a free space is a light cone. Now we add a periodic perturbation as depicted in Fig. 1.6(a) with an infinitesimal dielectric contrast between the rods and the surrounding space. This makes the cone fold into the first Brillouin zone due to the Bloch theorem. In Fig. 1.6(b) we show the projections of this folded cone in the directions Σ and Δ . The photonic states on the dispersion curves are degenerated at symmetric points (Γ , X , M). Some lines conserve their linear character and they will slightly curve when we increase the contrast between the rods and the surrounding medium: this will (at least partly) lift the degeneracy. Note, however, that some curves are not linear and they are quite flat even in the

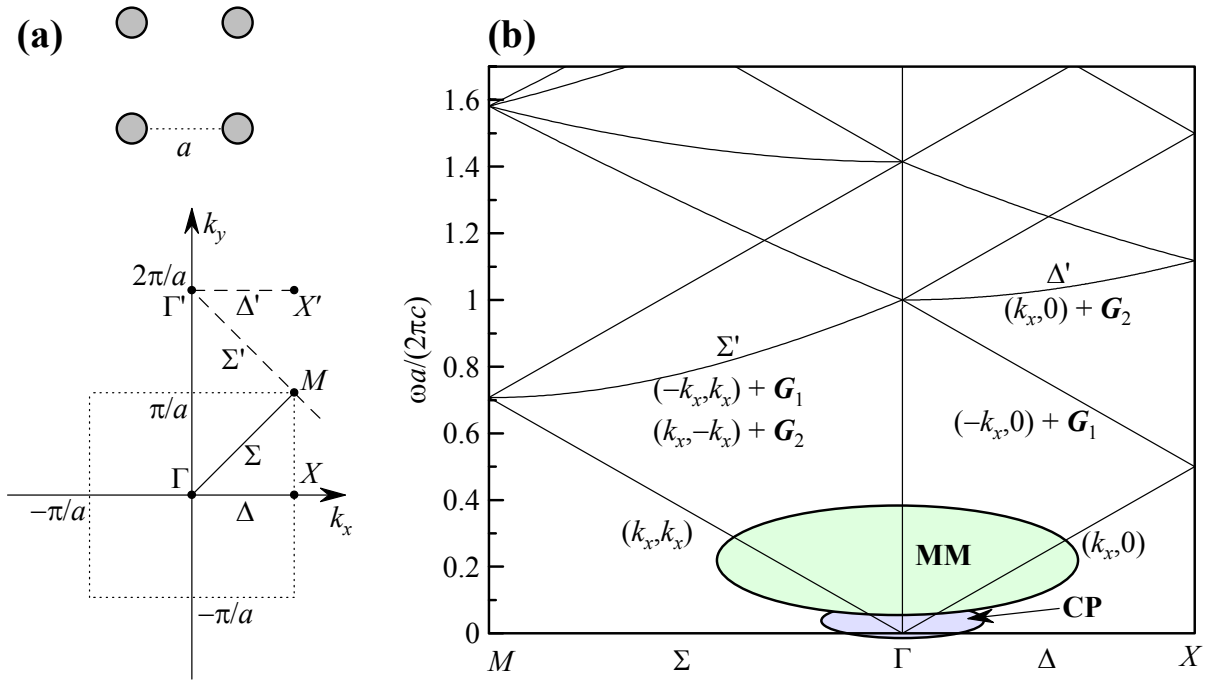


Figure 1.6: (a) Unit cell of a structure consisting of a square array of dielectric rods and the corresponding lattice in the reciprocal space. (b) Dispersion curves in the limit of an infinitesimal contrast between the rods and the surrounding space. The dispersion curves of electromagnetic radiation in a free space are just folded into the first Brillouin zone, see text for more details. MM: zone where the metamaterial behavior is expected if the elements of the photonic structure are individually resonant, CP: zone where the composite behavior is expected.

limit of zero contrast (e.g. Δ' , Σ'). Their origin is depicted in Fig. 1.6(a) by dashed lines; such lines do not pass through the origin of the reciprocal space. For example the dispersion of Δ' is written as:

$$\frac{\omega}{c} = \sqrt{k_x^2 + (2\pi/a)^2} \quad (1.34)$$

and the dispersion of Σ' reads:

$$\frac{\omega}{c} = \sqrt{k_x^2 + (2\pi/a - k_x)^2}. \quad (1.35)$$

As pointed out in the previous paragraph, these “flat” dispersion curves have a high density of states and low group velocity of propagation, *i.e.* features which are often exploited in the photonic crystals.

In Fig. 1.7 we show the dispersion curves calculated for a 2D photonic crystal composed of a medium with dielectric permittivity of 2.1 with cylindrical holes drilled into it (the figure is reproduced from [K. Sakoda, Optical Properties of Photonic Crystals, Springer Berlin 2001]). The various letters denoting the branches describe the symmetry of the modes and will be explained later in this textbook. The curves are directly comparable to those shown in Fig. 1.6(b). We observe the results of the coupling between the modes: the degeneracy is lifted in some cases and dispersion curves show anti-crossing behavior at some points; the similarity with Fig. 1.6(b) is quite apparent.

Fig. 1.8 shows an example of the transmission spectrum of a slab composed of this photonic crystal. The observed features directly correspond to the band structure along the Γ - X direction

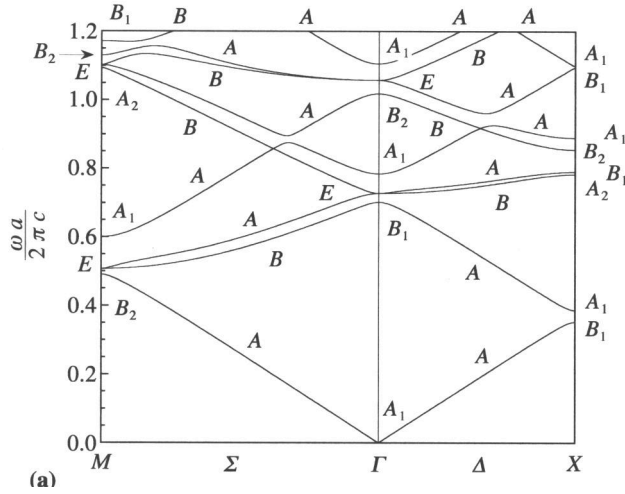


Figure 1.7: Dispersion relation of a 2D square lattice composed of dielectric material with $\varepsilon = 2.1$ with cylindrical holes drilled into it. E -polarization (electric field parallel to the rods and magnetic field in the plane); $r/a = 0.28$. Following [K. Sakoda, Optical Properties of Photonic Crystals, Springer Berlin 2001, p. 56].

in Fig. 1.7. The interference patterns observed in the frequency ranges (0.1–0.3) and (0.45–0.65) correspond to the linear parts of the lowest dispersion curves denoted as A . We observe here Fabry-Pérot like multiple reflections giving rise to interference maxima and minima. It means that here an effective refractive index can be defined for this particular direction of propagation corresponding to the slope of the dispersion curves. The frequency separation of individual maxima then corresponds to the density of states in a quasi-linear part of the dispersion curve. The first band gap opens between 0.35 and 0.4 (BZ boundary) and the second between 0.7 and 0.73 (BZ center). In the next part the spectrum features a very flat dispersion curve with a small group velocity and a high density of states (cf. very dense interference pattern in the spectrum between 0.73 and 0.8). A more complex spectrum at even higher frequencies is related to a higher complexity of the band structure (crossing bands, various small gaps etc.).

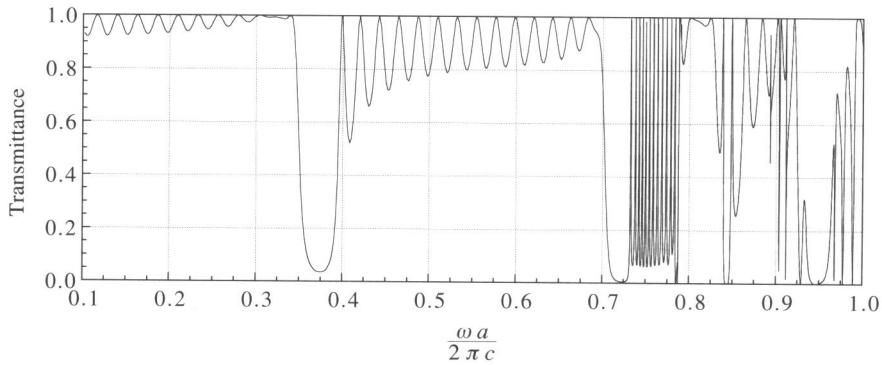


Figure 1.8: Transmission spectrum of a slab consisting of a photonic crystal composed of dielectric material with $\varepsilon = 2.1$ with cylindrical holes drilled in a 2D square lattice. Normal incidence, electric field polarized along the rods and propagation along the Γ - X direction. The corresponding band structure is shown in Fig. 1.7. Following [K. Sakoda, Optical Properties of Photonic Crystals, Springer Berlin 2001, p. 91].